

Rapid Communication

# Synthesis, crystal structure and spectroscopy properties of $\text{Na}_3AZr(\text{PO}_4)_3$ ( $A = \text{Mg}, \text{Ni}$ ) and $\text{Li}_{2.6}\text{Na}_{0.4}\text{NiZr}(\text{PO}_4)_3$ phosphates

M. Chakir<sup>a,\*</sup>, A. El Jazouli<sup>a</sup>, D. de Waal<sup>b</sup>

<sup>a</sup>LCMS, UFR Sciences des Matériaux Solides, Faculté des Sciences Ben M'Sik, UH2M, Avenue Idriss El Harti, BP 7955, Casablanca, Morocco

<sup>b</sup>Department of Chemistry, University of Pretoria, 0002 Pretoria, South Africa

Received 18 October 2005; received in revised form 6 March 2006; accepted 8 March 2006

Available online 19 April 2006

## Abstract

$\text{Na}_3AZr(\text{PO}_4)_3$  ( $A = \text{Mg}, \text{Ni}$ ) phosphates were prepared at 750 °C by coprecipitation route. Their crystal structures have been refined at room temperature from X-ray powder diffraction data using Rietveld method.  $\text{Li}_{2.6}\text{Na}_{0.4}\text{NiZr}(\text{PO}_4)_3$  was synthesized through ion exchange from the sodium analog. These materials belong to the Nasicon-type structure. Raman spectra of  $\text{Na}_3AZr(\text{PO}_4)_3$  ( $A = \text{Mg}, \text{Ni}$ ) phosphates present broad peaks in favor of the statistical distribution in the sites around  $\text{PO}_4$  tetrahedra. Diffuse reflectance spectra indicate the presence of octahedrally coordinated  $\text{Ni}^{2+}$  ions.

© 2006 Elsevier Inc. All rights reserved.

**Keywords:** Structure; Nasicon; X-ray diffraction; Raman

## 1. Introduction

Nasicon-type materials with general formula  $M_nA_2(\text{PO}_4)_3$  have been extensively studied in the context of various fields of solid state chemistry: solid electrolytes [1], electrode materials [2], low thermal expansion ceramics [3], etc. Their structure [4] consists of a three-dimensional network built up of  $\text{PO}_4$  tetrahedra sharing corners with  $\text{AO}_6$  octahedra. In this skeleton, there are two sites, usually labeled  $M(1)$  and  $M(2)$ . The  $M(1)$  site is an antiprism formed by the triangular faces of two  $\text{AO}_6$  octahedra along  $c$ -axis of the hexagonal cell. Thus the network of the  $\text{Na}_3A_2(\text{PO}_4)_3$  can be considered as made up of infinite ribbons of composition  $(\text{O}_3\text{AO}_3\text{MIO}_3\text{AO}_3)_\infty$  connected by  $\text{PO}_4$  tetrahedra. The  $M(2)$  sites are located between these ribbons in large cavities with a eight-fold coordination. The  $M(1)$  and  $M(2)$  sites may be completely empty as in  $\text{NbZr}(\text{PO}_4)_3$  [5], partially occupied as in  $\text{NaZr}_2(\text{PO}_4)_3$  [4],  $\text{Na}_3\text{CaTi}(\text{PO}_4)_3$  [6], and  $\text{Na}_3\text{MgTi}(\text{PO}_4)_3$  [7], or full as in  $\text{Na}_5\text{Ti}(\text{PO}_4)_3$  [8],  $\text{Na}_5\text{Zr}(\text{PO}_4)_3$  [9], and  $\text{Na}_{4.5}\text{Yb}_{1.5}(\text{PO}_4)_3$  [10]. Recently, a neutron diffraction investigation by Masquelier's group shows that in the two rhombohedral

Nasicon  $\text{Li}_3\text{Fe}_2(\text{PO}_4)_3$  and  $\text{Li}_3\text{V}_2(\text{PO}_4)_3$ , lithium ions are distributed on a new four-fold-coordinated site that they label  $M(3)$  [11,12]. In this site, the lithium atoms surround only the  $M(1)$  ( $3a$ ) site and are arranged in a tetrahedral environment.

The compound  $\text{Na}_3\text{MgZr}(\text{PO}_4)_3$  has been already prepared [13], but its structure has not been determined. Crystal data and ionic conductivity have been reported for the  $\text{Na}_{1+x}\text{Mg}_{x/2}\text{Zr}_{2-x/2}(\text{PO}_4)_3$  ( $0 \leq x \leq 2$ ) compositions prepared by solid-state reaction [14]. We showed recently by coprecipitation method that the solid solutions  $\text{Na}_{1+x}A_{x/2}\text{Zr}_{2-x/2}(\text{PO}_4)_3$  ( $A = \text{Mg}, \text{Ni}$ ) exist in the range of ( $0 \leq x \leq 3$ ) [15].

The present paper reports on the preparation of  $\text{Na}_3\text{MgZr}(\text{PO}_4)_3$  and  $\text{Na}_3\text{NiZr}(\text{PO}_4)_3$  by coprecipitation method, the refinement of their crystal structure from X-ray powder diffraction patterns and on their characterization by Raman and UV-visible spectroscopies. Synthesis and X-ray diffraction (XRD) results of a new  $\text{Li}_{2.6}\text{Na}_{0.4}\text{NiZr}(\text{PO}_4)_3$  phosphate are also reported.

## 2. Experimental

$\text{Na}_3AZr(\text{PO}_4)_3$  ( $A = \text{Mg}, \text{Ni}$ ) phosphates were obtained by coprecipitation route from  $\text{Na}_2\text{CO}_3(\text{I})$  dissolved in

\*Corresponding author. Fax: +212 22 70 46 75.

E-mail address: [fachakir@yahoo.fr](mailto:fachakir@yahoo.fr) (M. Chakir).

dilute nitric acid solution and aqueous solutions of  $(\text{ZrOCl}_2 \cdot 8\text{H}_2\text{O})$ (II),  $(\text{A}(\text{NO}_3)_2 \cdot 6\text{H}_2\text{O})$ (III) ( $A = \text{Mg}, \text{Ni}$ ) and  $(\text{NH}_4)_2\text{HPO}_4$ (IV) as starting materials (all solutions were prepared in stoichiometric proportions). A slow addition of (IV) in (I + II + III) mixture at room temperature induces the formation of a gel. After drying at  $60^\circ\text{C}$ , the resulting powder was progressively heated in air at  $200^\circ\text{C}$  (24 h),  $400^\circ\text{C}$  (24 h),  $600^\circ\text{C}$  (24 h) and  $750^\circ\text{C}$  (24 h) with intermitting regrinding. The powder of  $\text{Na}_3\text{MgZr}(\text{PO}_4)_3$  is white while that of  $\text{Na}_3\text{NiZr}(\text{PO}_4)_3$  is yellow.

$\text{Li}_{2.6}\text{Na}_{0.4}\text{NiZr}(\text{PO}_4)_3$  can be obtained from  $\text{Na}_3\text{NiZr}(\text{PO}_4)_3$  after ion exchange in molten  $\text{LiNO}_3$ . To favor ion exchange, the weight ratio  $\text{LiNO}_3/\text{Na}_3\text{NiZr}(\text{PO}_4)_3$  was set to  $>10$ , and the mixture was maintained for 3 h at  $300^\circ\text{C}$ . The final ion-exchange solid was washed repeatedly with distilled water to eliminate the  $(\text{Li}, \text{Na})\text{NO}_3$  compounds before drying overnight at  $60^\circ\text{C}$ . Chemical analysis revealed that the  $\text{Na}^+ \leftrightarrow \text{Li}^+$  ion-exchange was not complete: the final product presented the formula  $\text{Li}_{2.6}\text{Na}_{0.4}\text{NiZr}(\text{PO}_4)_3$ . Its purity and lattice parameters determination were carefully monitored by XRD on a Panalytical X'Pert PRO diffractometer (CoK $\alpha$  radiation). Diffraction data of  $\text{Na}_3\text{AZr}(\text{PO}_4)_3$  ( $A = \text{Mg}, \text{Ni}$ ) phosphates were collected at room temperature on a Siemens D 5000 diffractometer.

Raman spectra were recorded using a Dilor XY Raman microprobe. The samples were excited with the 514.5 nm line of an argon ion laser (Coherent model Innova 300). The spectral resolution was  $3\text{ cm}^{-1}$ , the laser output power 110 mW, and the integration time 30 s. Absorption spectra were recorded using a double monochromator Cary 2400 spectrometer at 300 K.

### 3. Results and discussion

#### 3.1. Rietveld refinement and structure study of $\text{Na}_3\text{AZr}(\text{PO}_4)_3$ ( $A = \text{Mg}, \text{Ni}$ )

The X-ray powder diffraction data show that  $\text{Na}_3\text{AZr}(\text{PO}_4)_3$  ( $A = \text{Mg}, \text{Ni}$ ) phosphates crystallize in the trigonal system (S. G.  $R\bar{3}c$ ). Assuming that  $\text{Na}_3\text{MgZr}(\text{PO}_4)_3$  and

$\text{Na}_3\text{NiZr}(\text{PO}_4)_3$  belong to the Nasicon family, the Zr(A), P and O atoms are in the (12c), (18e) and (36f) Wyckoff positions, respectively, of the  $R\bar{3}c$  space group. The initial atomic coordinates used for the refinement of the crystal structure of  $\text{Na}_3\text{MgZr}(\text{PO}_4)_3$  were those of  $\text{Na}_{4.5}\text{Yb}_{1.5}(\text{PO}_4)_3$  [10].  $\text{Na}_3\text{MgZr}(\text{PO}_4)_3$  was then used as a model to refine the structure of  $\text{Na}_3\text{NiZr}(\text{PO}_4)_3$ . Na atoms were assumed to occupy the  $M(1)$  and  $M(2)$  sites. In the first step, Na occupy fully the  $M(1)$  site and the excess of sodium (two atoms) was located in the  $M(2)$  site (18e). These refinements lead to a rather good agreement between the experimental and calculated XRD patterns and to follow reliability factors [ $R_p = 11\%$ ,  $R_{wp} = 14\%$  and  $R_B = 6\%$  for  $\text{Na}_3\text{MgZr}(\text{PO}_4)_3$ , and  $R_p = 8\%$ ,  $R_{wp} = 11\%$  and  $R_B = 5\%$  for  $\text{Na}_3\text{NiZr}(\text{PO}_4)_3$ ]. In the second step, the occupancies of Na(1) and Na(2) sites were allowed to vary, but the total sodium contents were constrained to 3. The result of these refinements show clearly a partial occupancy of  $M(1)$  and  $M(2)$  sites. The crystallographic formulas are  $[\text{Na}_{2.11}\square_{0.89}]_{M2}[\text{Na}_{0.89}\square_{0.11}]_{M1}[\text{MgZr}]_A(\text{PO}_4)_3$  and  $[\text{Na}_{2.09}\square_{0.91}]_{M2}[\text{Na}_{0.91}\square_{0.09}]_{M1}[\text{NiZr}]_A(\text{PO}_4)_3$ . The same distribution was already shown for  $\text{Na}_2\text{SnFe}(\text{PO}_4)_3$  phosphate [16]. On the other hand, and in order to confirm the cationic distributions already obtained, the structural refinement of  $\text{Na}_3\text{AZr}(\text{PO}_4)_3$  ( $A = \text{Mg}, \text{Ni}$ ) was undertaken assuming that Na atoms were distributed also in  $M(3)$  sites. This refinement leads to high displacement parameters and/or to unacceptable P–O distances values.

The experimental conditions and the results of the refinements as well as different structural parameters are given in Tables 1 and 2. Figs. 1 and 2 show observed, calculated and different X-ray profiles for  $\text{Na}_3\text{MgZr}(\text{PO}_4)_3$  and  $\text{Na}_3\text{NiZr}(\text{PO}_4)_3$ .

The structure of  $\text{Na}_3\text{AZr}(\text{PO}_4)_3$  ( $A = \text{Mg}, \text{Ni}$ ) is based on a three-dimensional framework of  $\text{PO}_4$  tetrahedra and  $(\text{Zr}/A)\text{O}_6$  octahedra sharing corners (Fig. 3).  $\text{Zr}^{4+}$  and  $A^{2+}$  ions occupy statistically the 12c sites.  $\text{Na}^+$  cations occupy partially the  $M(1)$  and  $M(2)$  sites. Zr/A ( $A = \text{Mg}, \text{Ni}$ ) atoms are displaced from the center of the octahedron due to the  $\text{Na}^+ - \text{Zr}^{4+}/A^{2+}$  repulsions. Consequently the Zr/A–O(2) distance ( $2.097\text{ \AA}$  for Zr/Mg and  $2.100\text{ \AA}$  for

Table 1  
Conditions and results of the Rietveld refinement of  $\text{Na}_3\text{AZr}(\text{PO}_4)_3$  ( $A = \text{Mg}, \text{Ni}$ )

Composition	$\text{Na}_3\text{MgZr}(\text{PO}_4)_3$	$\text{Na}_3\text{NiZr}(\text{PO}_4)_3$
Wavelength ( $\text{\AA}$ )	$\lambda\kappa\alpha_1 = 1.5406$ ; $\lambda\kappa\alpha_2 = 1.5444$	
Step width ( $^\circ 2\theta$ ); angular range ( $^\circ$ )	0.04; 10–100	0.02; 10–100
Zero point ( $^\circ 2\theta$ )	0.162(1)	–0.065(2)
Pseudo-Voigt function	$\eta = 0.522(4)$	$\eta = 0.469(2)$
Half-width parameters: $U, V, W$	0.238(1), –0.099(1), 0.051(1)	0.196(3), –0.067(2), 0.033(2)
Number of reflections	398	363
System; space group; Z	Trigonal; $R\bar{3}c$ ; 6	
$a$ ( $\text{\AA}$ ); $c$ ( $\text{\AA}$ )	8.9095(4); 22.255(1)	8.8909(4); 22.225(1)
$V$ ( $\text{\AA}^3$ )	1529.9(1)	1521.5(1)
$R_B$ ; $R_p$ ; $R_{wp}$	0.06; 0.12; 0.13	0.05; 0.11; 0.13

Table 2  
Atomic coordinates and isotropic temperature factors in  $\text{Na}_3AZr(\text{PO}_4)_3$  ( $A = \text{Mg}, \text{Ni}$ )

Atom	Wyckoff site	$x$	$y$	$z$	$B_{\text{iso}} (\text{\AA}^2)$	Occ.
<i>Na<sub>3</sub>MgZr(PO<sub>4</sub>)<sub>3</sub></i>						
Zr/Mg	12c	0	0	0.1474(1)	0.5(1)	1
Na(1)	6b	0	0	0	4.8(6)	0.89(2)
Na(2)	18e	0.6400(9)	0	0.2500	5.4(8)	0.703(1)
P	18e	0.2935(4)	0	0.2500	1.1(3)	1
O(1)	36f	0.1852(6)	−0.0250(6)	0.1942(2)	0.8(4)	1
O(2)	36f	0.1926(5)	0.1725(6)	0.0883(3)	1.0(5)	1
<i>Na<sub>3</sub>NiZr(PO<sub>4</sub>)<sub>3</sub></i>						
Zr/Ni	12c	0	0	0.1474(1)	0.9(2)	1
Na(1)	6b	0	0	0	4.2(7)	0.91(1)
Na(2)	18e	0.6340(14)	0	0.2500	6.3(3)	0.697(1)
P	18e	0.2934(5)	0	0.2500	0.9(3)	1
O(1)	36f	0.1865(9)	−0.0249(10)	0.1941(3)	1.1(4)	1
O(2)	36f	0.1908(7)	0.1717(8)	0.0872(3)	1.1(4)	1

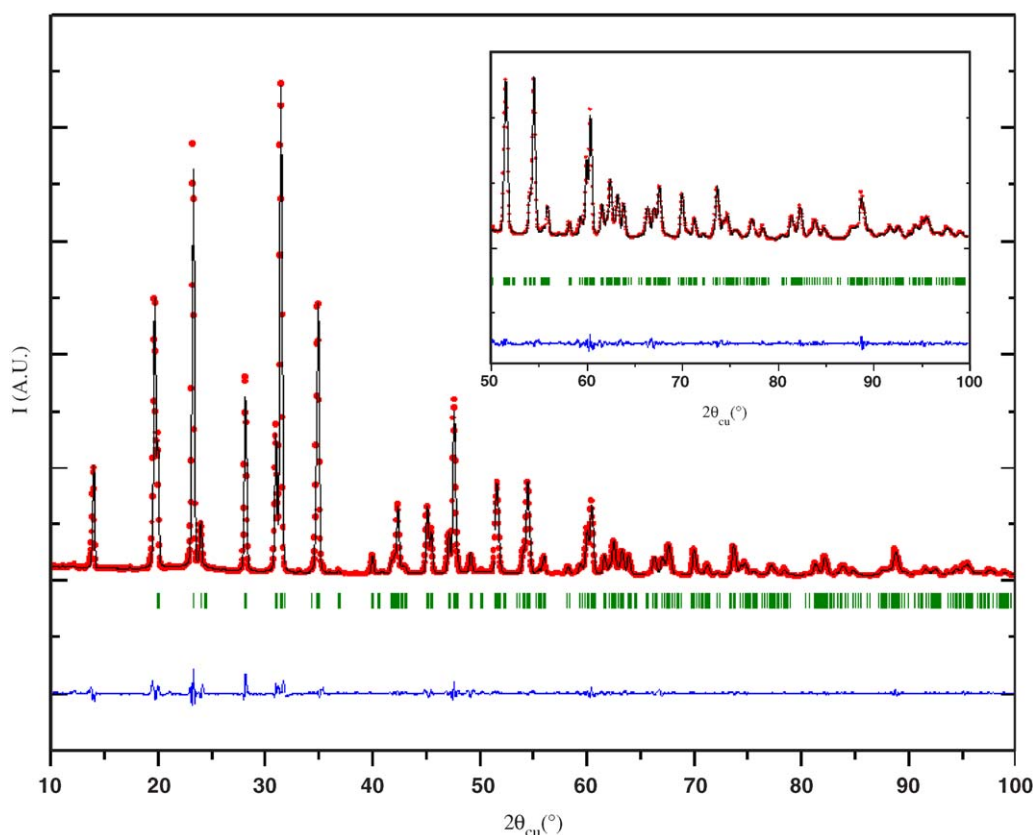


Fig. 1. Observed (...), calculated (—) and different powder diffraction patterns of  $\text{Na}_3\text{MgZr}(\text{PO}_4)_3$ .

Zr/Ni), neighboring the sodium Na(1), is slightly greater than the Zr/A–O(1) distance (2.055 Å for Zr/Mg and 2.059 Å for Zr/Ni) (Tables 3 and 4). The average Zr/A–O distances (2.076 Å for Zr/Mg and 2.080 Å for Zr/Ni) are slightly smaller than the values calculated from the ionic radii (2.12 Å for Zr/Mg and 2.11 Å for Zr/Ni) [17]. The O–(Zr/A)–O angles vary between 84.8° and 171.5° for Zr/Mg and between 83.7° and 170.6° for Zr/Ni. The angles implying the shortest bonds are superior to those involving the longest ones as a consequence of the O–O repulsions

which are stronger for O(1)–O(1) than for O(1)–O(2) and O(2)–O(2). Zr/A–Zr/A distance along  $c$ -axis (4.566 Å for Mg and 4.559 Å for Ni) is inferior to the Zr–Zr distance in  $\text{NaZr}_2(\text{PO}_4)_3$  (4.752 Å) due to the cationic repulsions between ions in 12c sites. These repulsions are stronger in  $\text{NaZr}_2(\text{PO}_4)_3$  (charge of  $\text{Zr}^{4+} = 4$ ) than in  $\text{Na}_3AZr(\text{PO}_4)_3$  (mean charge of  $\text{Zr}^{4+}/A^{2+} = 3$ ).

The P–O distances values [(1.519; 1.532 Å) for  $\text{Na}_3\text{MgZr}(\text{PO}_4)_3$  and (1.512; 1.540 Å) for  $\text{Na}_3\text{NiZr}(\text{PO}_4)_3$ ] are close to those typically found in Nasicon-like

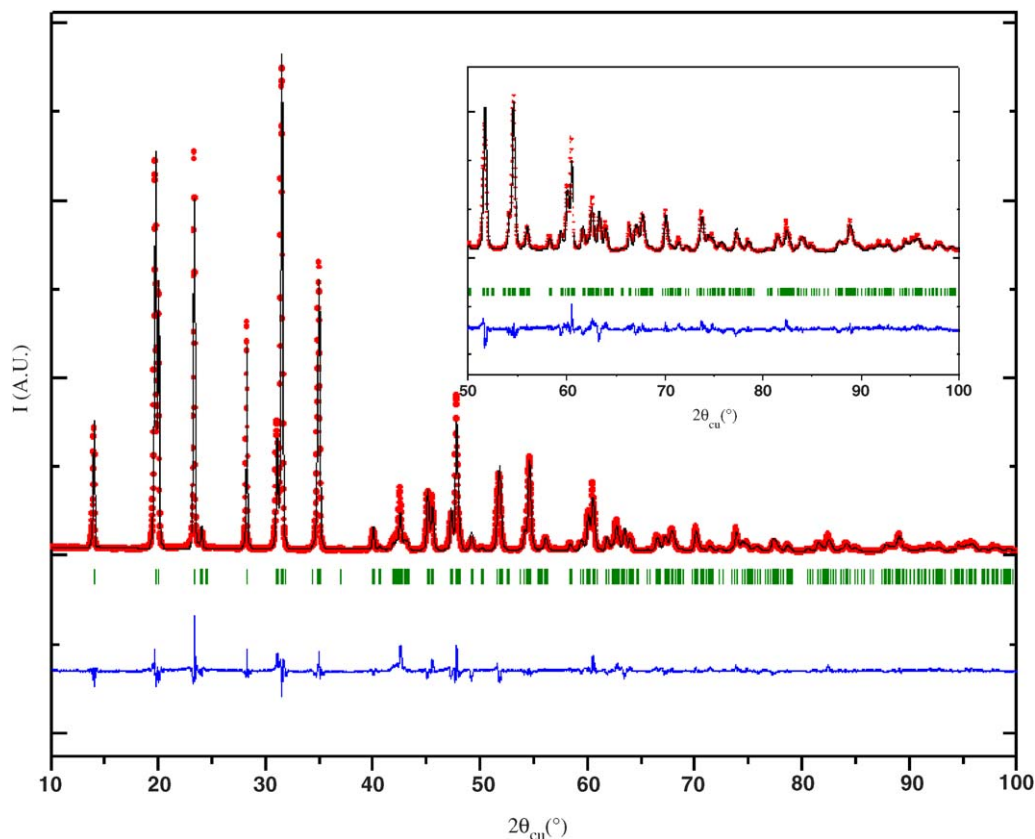


Fig. 2. Observed (...), calculated (—) and different powder diffraction patterns of  $\text{Na}_3\text{NiZr}(\text{PO}_4)_3$ .

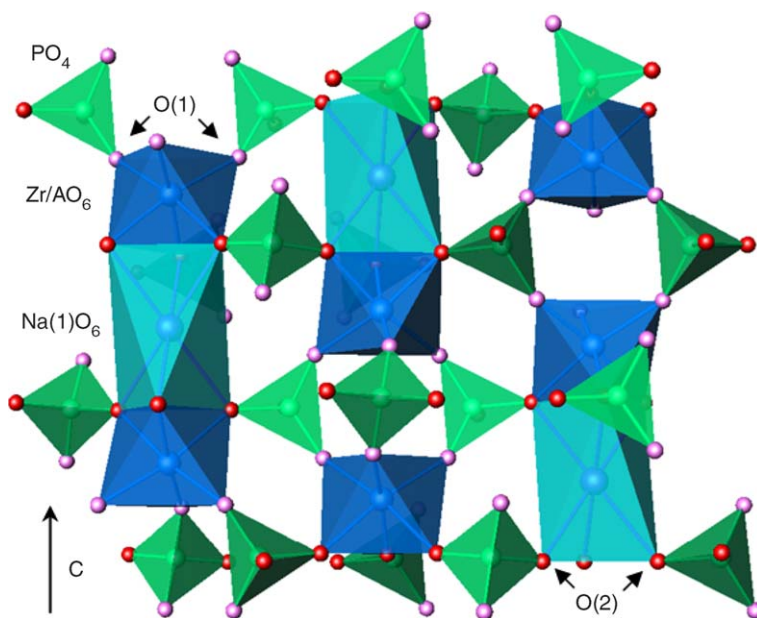


Fig. 3. Structure of  $\text{Na}_3\text{AZr}(\text{PO}_4)_3$  ( $A = \text{Mg}, \text{Ni}$ ) phosphates.

phosphates. O–P–O angles vary from  $106.4^\circ$  to  $111.7^\circ$  for  $\text{Na}_3\text{MgZr}(\text{PO}_4)_3$  and from  $105.6^\circ$  to  $112.5^\circ$  for  $\text{Na}_3\text{NiZr}(\text{PO}_4)_3$ . The Na(1) atoms occupy the center of the  $M(1)$  site. Na(1)–O(2) distance (Tables 3 and 4) ( $2.555 \text{ \AA}$  for  $\text{Na}_3\text{MgZr}(\text{PO}_4)_3$  and  $2.525 \text{ \AA}$  for  $\text{Na}_3\text{NiZr}(\text{PO}_4)_3$ ) is larger

than the calculated one ( $2.42 \text{ \AA}$ ) from the ionic radii [17]. The Na(2) atoms, located in the  $M(2)$  site, are surrounded by eight oxygen atoms, the Na(2)–O distances vary from  $2.449$  to  $2.872 \text{ \AA}$  for  $\text{Na}_3\text{MgZr}(\text{PO}_4)_3$  and from  $2.457$  to  $2.909 \text{ \AA}$  for  $\text{Na}_3\text{NiZr}(\text{PO}_4)_3$ . The ionic character of the

Table 3  
Bond distances and angles for Na<sub>3</sub>MgZr(PO<sub>4</sub>)<sub>3</sub>

Bond distances (Å)		Angles (deg)	
(Zr/Mg)–O(1) × 3	2.055(5)	O(1)–(Zr/Mg)–O(1)	96.6(3)
(Zr/Mg)–O(2) × 3	2.097(5)	O(1)–(Zr/Mg)–O(2)	88.4(3); 89.4(3); 171.5(4)
P–O(1) × 2	1.519(5)	O(2)–(Zr/Mg)–O(2)	84.8(3)
P–O(2) × 2	1.532(5)	O(1)–P–O(1)	111.6(4)
Na(1)–O(2) × 6	2.555(4)	O(1)–P–O(2)	106.4(5); 111.7(5)
Na(2)–O(1) × 2	2.872(8)	O(2)–P–O(2)	108.7(4)
Na(2)–O(1) × 2	2.697(5)	O(2)–Na(1)–O(2)	67.2(2); 112.7(3); 180.0(4)
Na(2)–O(2) × 2	2.524(8)	O(1)–Na(2)–O(1)	82.4(2); 85.8(3); 111.6(3); 157.2(3)
Na(2)–O(2) × 2	2.449(4)	O(1)–Na(2)–O(2)	53.9(2); 67.3(2); 114.8(3); 151.6(4)
		O(2)–Na(2)–O(2)	59.1(3); 69.3(3); 128.4(4); 162.1(3)

Table 4  
Bond distances and angles for Na<sub>3</sub>NiZr(PO<sub>4</sub>)<sub>3</sub>

Bond distances (Å)		Angles (deg)	
(Zr/Ni)–O(1) × 3	2.059(8)	O(1)–(Zr/Ni)–O(1)	96.8(6)
(Zr/Ni)–O(2) × 3	2.100(7)	O(1)–(Zr/Ni)–O(2)	88.8(1); 89.9(1); 170.6(3)
P–O(1) × 2	1.512(8)	O(2)–(Zr/Ni)–O(2)	83.7(2)
P–O(2) × 2	1.540(7)	O(1)–P–O(1)	112.4(2)
Na(1)–O(2) × 6	2.525(7)	O(1)–P–O(2)	105.6(2); 112.5(2)
Na(2)–O(1) × 2	2.909(7)	O(2)–P–O(2)	108.1(8)
Na(2)–O(1) × 2	2.677(12)	O(2)–Na(1)–O(2)	67.4(5); 112.5(5); 180.0
Na(2)–O(2) × 2	2.457(7)	O(1)–Na(2)–O(1)	81.4(6); 85.1(1); 110.6(7); 159.6(6)
Na(2)–O(2) × 2	2.463(13)	O(1)–Na(2)–O(2)	53.2(4); 69.7(4); 114.6(6); 152.4(7)
		O(2)–Na(2)–O(2)	60.8(3); 69.4(5); 130.2(5); 160.3(1)

Na–O bonds explains the high conductivity found for Na<sub>3</sub>MgZr(PO<sub>4</sub>)<sub>3</sub> [14], and the values of isotropic temperature factors obtained for Na atoms in *M*(1) and *M*(2) sites.

Calculated valences ( $S_i = \sum \exp[(R_{ij} - d_{ij})/b]$  with  $b = 0.37 \text{ \AA}$ ) based on bond strength analysis [18] [P: 5.14, Zr: 4.01, Mg: 2.12, Na(1): 0.80, Na(2): 0.92 for Na<sub>3</sub>MgZr(PO<sub>4</sub>)<sub>3</sub> and P: 4.94, Zr: 4.11, Ni: 1.91, Na(1): 0.86, Na(2): 0.94 for Na<sub>3</sub>NiZr(PO<sub>4</sub>)<sub>3</sub>] are in good agreement with the expected formal oxidation states of P<sup>5+</sup>, Zr<sup>4+</sup>, Mg<sup>2+</sup>, Ni<sup>2+</sup> and Na<sup>+</sup>.

### 3.2. Crystallochemical study

The X-ray powder patterns of Na<sub>3</sub>AZr(PO<sub>4</sub>)<sub>3</sub> ( $A = \text{Mg, Ni}$ ) can be indexed assuming a hexagonal cell parameters:  $a_h = 8.9095(4) \text{ \AA}$ ;  $c_h = 22.255(1) \text{ \AA}$  for Na<sub>3</sub>MgZr(PO<sub>4</sub>)<sub>3</sub> and  $a_h = 8.8909(4) \text{ \AA}$ ;  $c_h = 22.225(1) \text{ \AA}$  for Na<sub>3</sub>NiZr(PO<sub>4</sub>)<sub>3</sub>. All of the observed reflections are compatible with the  $R\bar{3}c$  space group. Contrary to the pure sodium composition, Li<sub>2.6</sub>Na<sub>0.4</sub>NiZr(PO<sub>4</sub>)<sub>3</sub> X-ray pattern was indexed in  $R\bar{3}c$  space group. Indeed, XRD pattern (Fig. 4) clearly shows reflections such as (102) ( $2\theta_{\text{CoK}\alpha} \approx 16.5^\circ$ ) and (303) ( $2\theta_{\text{CoK}\alpha} \approx 44.9^\circ$ ) which are normally forbidden in the  $R\bar{3}c$  space group. The cell parameters are  $a_h = 8.4716(2) \text{ \AA}$  and  $c_h = 23.054(1) \text{ \AA}$ .

In Nasicon family, the  $a_h$ -parameter depends on the ribbon diameter (i.e. is a function of the  $A$  size) and on the interribbon distance (which is related to the amount and to size of the alkali cations in the *M*(2)

or *M*(3) sites). The comparison of the  $a_h$ -parameters of Na<sub>3</sub>NiZr(PO<sub>4</sub>)<sub>3</sub> ( $a_h = 8.8909 \text{ \AA}$ ), and Li<sub>2.6</sub>Na<sub>0.4</sub>NiZr(PO<sub>4</sub>)<sub>3</sub> ( $a_h = 8.4716 \text{ \AA}$ ), which should have the same ribbon diameter, clearly illustrates the influence of Li<sup>+</sup> insertion in the *M*(2) or *M*(3) sites; the decrease of  $a_h$  parameter, when sodium is replaced by lithium in Na<sub>3</sub>NiZr(PO<sub>4</sub>)<sub>3</sub>, is related to the size of Li<sup>+</sup> ( $r_{\text{Li}^+} = 0.74 \text{ \AA}$ ) which is smaller than that of Na<sup>+</sup> ion ( $r_{\text{Na}^+} = 1.02 \text{ \AA}$ ) [17]. These results are interpreted based on the fact that, in Li<sub>2.6</sub>Na<sub>0.4</sub>NiZr(PO<sub>4</sub>)<sub>3</sub> phosphate, Na atoms are placed in *M*(1) site and Li atoms occupy the *M*(2) or *M*(3) sites. It should be noticed that this hypothesis was already verified for Li<sub>1.6</sub>Na<sub>0.4</sub>TiM(PO<sub>4</sub>)<sub>3</sub> ( $M = \text{Fe, Cr}$ ) Nasicon phases [19]. The  $c_h$ -parameter increases as Li substitutes for Na [ $c_h = 22.225 \text{ \AA}$  for Na<sub>3</sub>NiZr(PO<sub>4</sub>)<sub>3</sub> and  $c_h = 23.054 \text{ \AA}$  for Li<sub>2.6</sub>Na<sub>0.4</sub>NiZr(PO<sub>4</sub>)<sub>3</sub>]. This behavior results mainly from the Na<sup>+</sup> amount present in the *M*(1) sites which decreases the O(2)–O(2) repulsions along  $c$ -axis. The small difference of  $c_h$ -parameters of Na<sub>3</sub>AZr(PO<sub>4</sub>)<sub>3</sub> ( $A = \text{Mg, Ni}$ ) phosphates, can be explained by the slight difference in ionic radii between Mg<sup>2+</sup> (0.72 Å) and Ni<sup>2+</sup> (0.70 Å) in octahedral environments.

### 3.3. Raman investigation

Vibrational spectra have been recorded for all the compositions of the Na<sub>1+x</sub>A<sub>x/2</sub>Zr<sub>2-x/2</sub>(PO<sub>4</sub>)<sub>3</sub> ( $A = \text{Mg, Ni}$ ) ( $0 \leq x \leq 3$ ) series and will be published elsewhere [20]. Here we summarized the results obtained for

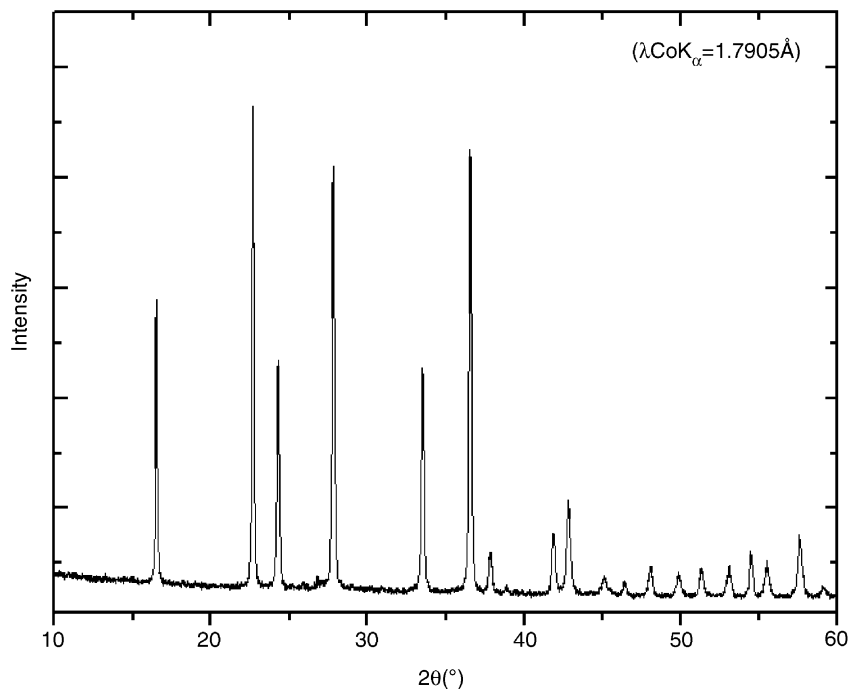


Fig. 4. X-ray diffraction pattern of  $\text{Li}_{2.6}\text{Na}_{0.4}\text{NiZr}(\text{PO}_4)_3$ .

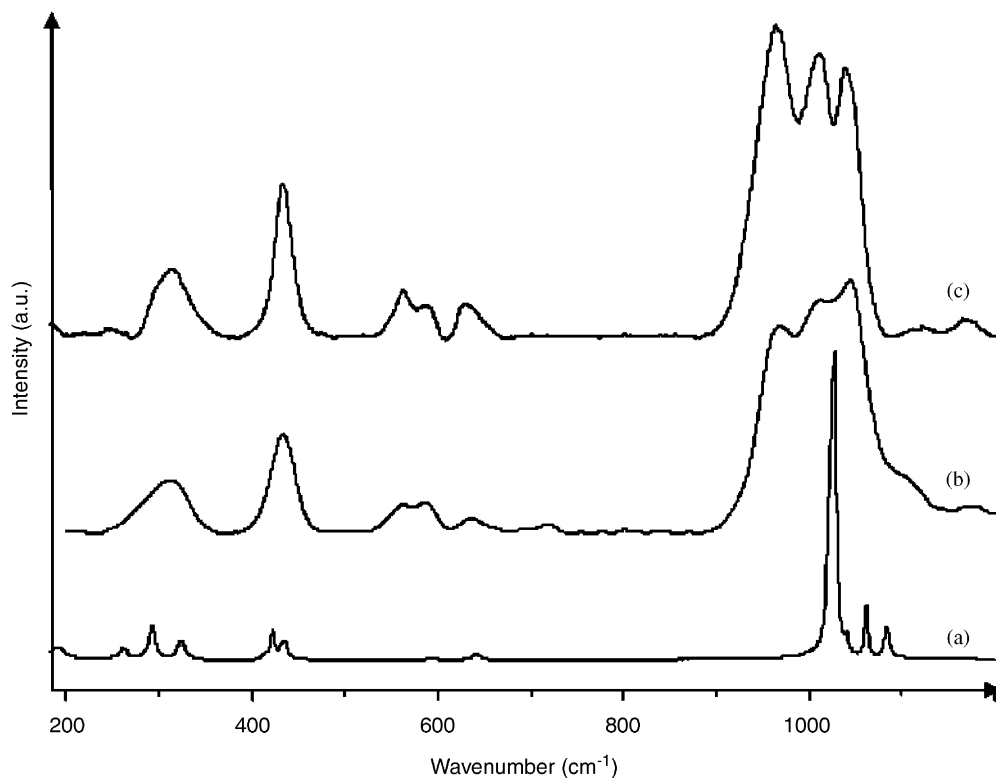


Fig. 5. Raman spectra of  $\text{NaZr}_2(\text{PO}_4)_3$  (a),  $\text{Na}_3\text{NiZr}(\text{PO}_4)_3$  (b) and  $\text{Na}_3\text{MgZr}(\text{PO}_4)_3$  (c).

$\text{Na}_3AZr(\text{PO}_4)_3$  ( $A = \text{Mg}, \text{Ni}$ ) compositions. Fig. 5 shows their Raman spectra. The high frequency part ( $900\text{--}1200\text{ cm}^{-1}$ ) of these spectra corresponds to the stretching vibrations of the  $\text{PO}_4$  tetrahedra and exhibits six peaks (Fig. 6) in good agreement with results of the factor group analysis of  $R\bar{3}c$ . The peaks observed between 700 and

$400\text{ cm}^{-1}$  are assigned to the P–O bending vibrations, the predicted ones are eight. The peaks situated below  $400\text{ cm}^{-1}$  are attributed to the external modes.

The peaks observed for  $\text{Na}_3AZr(\text{PO}_4)_3$  ( $A = \text{Mg}, \text{Ni}$ ) are broader than those obtained for  $\text{NaZr}_2(\text{PO}_4)_3$  [15,21]. In all these phosphates the  $\text{PO}_4$  tetrahedra are linked by corners

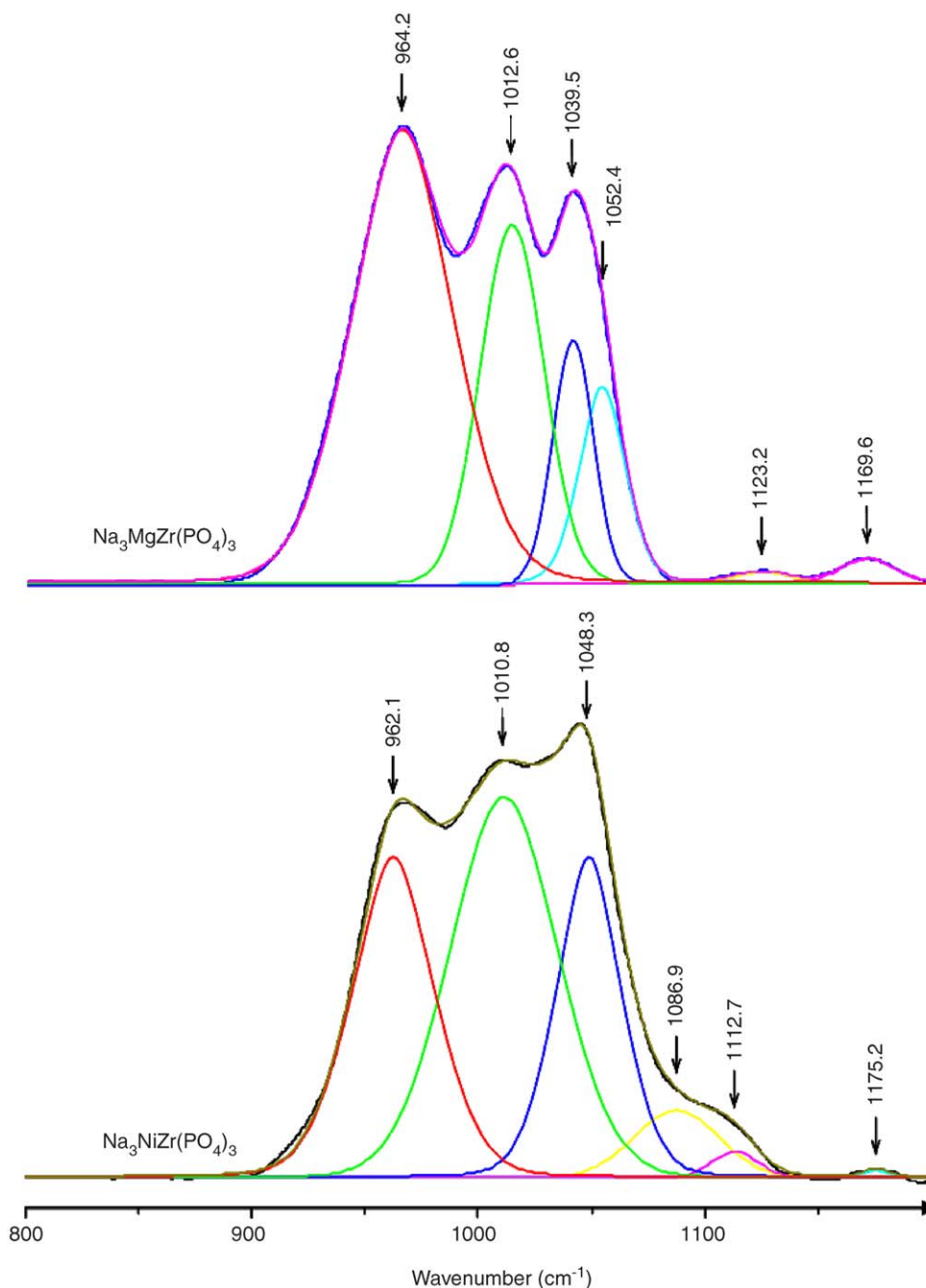


Fig. 6. Raman spectra of  $\text{Na}_3\text{AZr}(\text{PO}_4)_3$  ( $A = \text{Mg}, \text{Ni}$ ) (range of 800–1200  $\text{cm}^{-1}$ ).

to  $\text{Zr}/\text{AO}_6$  ( $A = \text{Mg}, \text{Ni}$ ),  $\text{Na}(1)\text{O}_6$  and  $\text{Na}(2)\text{O}_8$  polyhedra. In  $\text{NaZr}_2(\text{PO}_4)_3$  the octahedral site of the framework (12c) is occupied by  $\text{Zr}^{4+}$  only,  $M(1)$  site is totally occupied by  $\text{Na}^+$  and  $M(2)$  site is totally empty, so there is no disorder around the  $\text{PO}_4$  tetrahedra and the Raman peaks are very sharp. In  $\text{Na}_3\text{AZr}(\text{PO}_4)_3$  ( $A = \text{Mg}, \text{Ni}$ ) the statistical distribution of  $\text{A}^{2+}/\text{Zr}^{4+}$  and  $\text{Na}^+$  in 12c and  $M(2)$  sites, respectively, induces a disorder around  $\text{PO}_4$  tetrahedra and explains the very broad Raman peaks observed for these phosphates.

### 3.4. Optical properties

Fig. 7 presents the diffuse reflectance spectra of  $\text{Na}_3\text{AZr}(\text{PO}_4)_3$  ( $A = \text{Mg}, \text{Ni}$ ). The strong band observed at high energy, for both compounds, is due to the electronic transfer from oxygen to zirconium. The optical energy gap values are 4.96 eV for  $\text{Na}_3\text{NiZr}(\text{PO}_4)_3$  and 5.06 eV for  $\text{Na}_3\text{MgZr}(\text{PO}_4)_3$ . These results are in the range usually found for the isostructural phosphate  $\text{NaZr}_2(\text{PO}_4)_3$  (5.06 eV) [22]. The other bands situated in the visible and

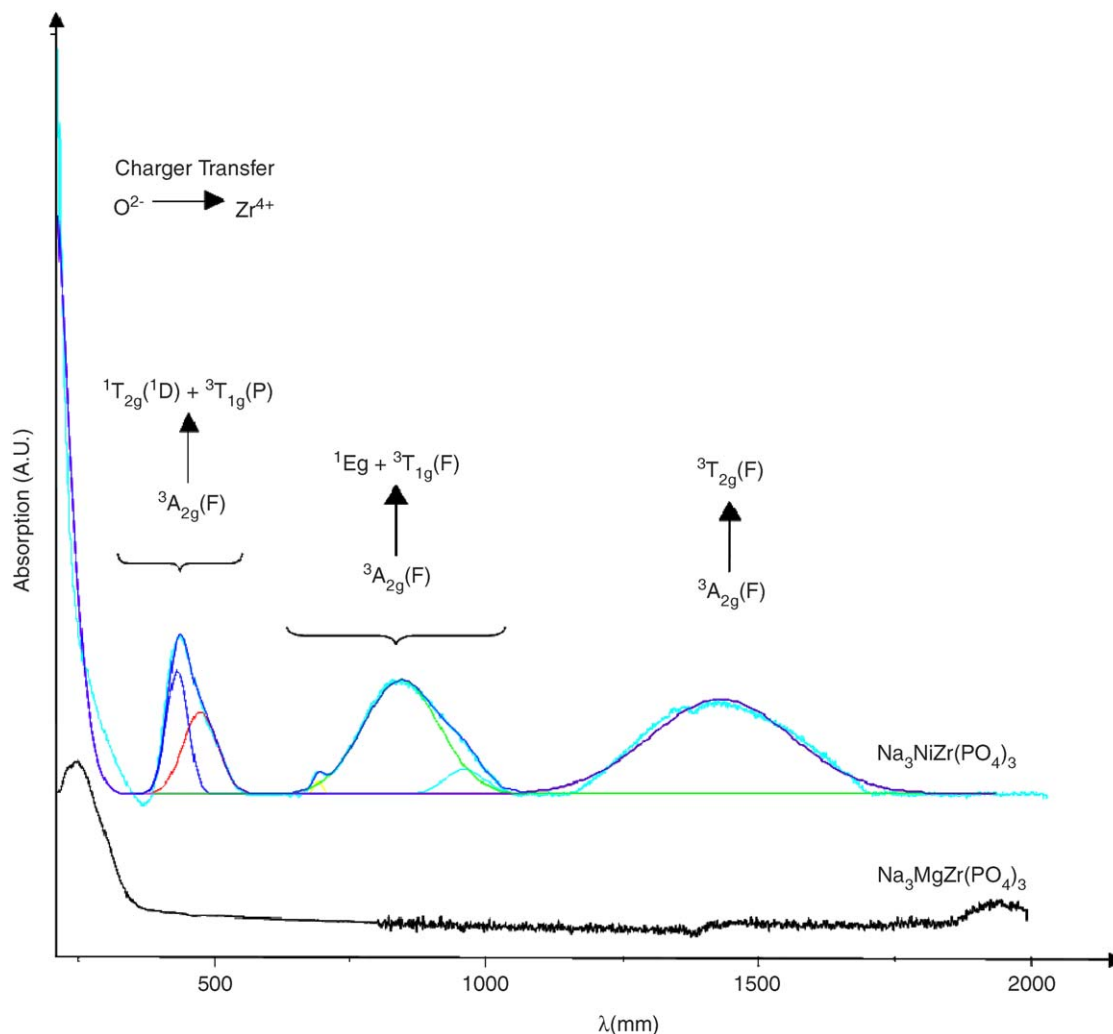


Fig. 7. Diffuse reflectance spectra of  $\text{Na}_3\text{AZr}(\text{PO}_4)_3$  ( $A = \text{Mg}, \text{Ni}$ ).

Table 5  
Experimental and calculated energies of  $\text{Ni}^{2+}$  transitions in  $\text{Na}_3\text{NiZr}(\text{PO}_4)_3$

Transition	Energy ( $\text{cm}^{-1}$ )	
	Obs.	Calc.
${}^3A_{2g}(\text{F}) \rightarrow {}^3T_{2g}(\text{F})$	6997	7000
${}^3A_{2g}(\text{F}) \rightarrow {}^3T_{1g}(\text{F})$	11,889	11,668
${}^3A_{2g}(\text{F}) \rightarrow {}^1E_g$	14,513	14,577
${}^3A_{2g}(\text{F}) \rightarrow {}^1T_{2g}({}^1D)$	21,186	20,618
${}^3A_{2g}(\text{F}) \rightarrow {}^3T_{1g}(\text{P})$	23,255	24,630

infrared domains, observed only in  $\text{Na}_3\text{NiZr}(\text{PO}_4)_3$ , are due to  $d-d$  transitions of  $\text{Ni}^{2+}$  in octahedral site. Three broad absorption bands ascribed to the spin-allowed transitions  ${}^3A_{2g} \rightarrow {}^3T_{2g}(\text{F})$ ,  ${}^3T_{1g}(\text{F})$ , and  ${}^3T_{1g}(\text{P})$  were observed at the following frequencies:  $\nu_1 = 6997$ ,  $\nu_2 = 11,889$  and  $\nu_3 = 23,255 \text{ cm}^{-1}$ . The spin-forbidden transitions  ${}^3A_{2g} \rightarrow {}^1E_g$ , and  ${}^1T_{2g}$  were also observed at  $\nu_4 = 14,513$  and  $\nu_5 = 21,186 \text{ cm}^{-1}$ . Table 5 compares the value of the observed and calculated energies. The value of the

ligands field parameter ( $Dq$ ) and Racah parameter ( $B$ ), calculated by fitting the experimental frequencies to an energy-level diagram for octahedral  $d^8$  systems [23], are  $Dq = 700 \text{ cm}^{-1}$  and  $B = 791 \text{ cm}^{-1}$  (for free ion,  $B(\text{Ni}^{2+})$  is  $1041 \text{ cm}^{-1}$ ). These values indicate a weak crystal field for  $\text{Ni}^{2+}$  and a covalent character of Ni–O bond in good agreement with structural results which showed that  $\text{Ni}^{2+}$  ions are located in the framework  $[\text{NiZr}(\text{PO}_4)_3]$ .

#### 4. Conclusion

A new phosphates  $\text{Li}_{2.6}\text{Na}_{0.4}\text{NiZr}(\text{PO}_4)_3$  and  $\text{Na}_3\text{NiZr}(\text{PO}_4)_3$  have been obtained, respectively, by ion exchange and coprecipitation routes. Structures of  $\text{Na}_3\text{AZr}(\text{PO}_4)_3$  ( $A = \text{Mg}, \text{Ni}$ ) have been refined from X-ray powder diffraction using Rietveld method. The latter phosphates belong to the Nasicon family and crystallize in the  $R\bar{3}c$  space group.  $A^{2+}$  ( $A = \text{Mg}, \text{Ni}$ ) and  $\text{Zr}^{4+}$  cations are statistically distributed in the octahedral sites (12c) of the framework. Na atoms occupy partially  $M(1)$  and  $M(2)$  sites. Raman spectra of these phosphates present broad peaks due to the statistical occupation of the sites



(12c,  $M(1)$  and  $M(2)$ ) around  $\text{PO}_4$  tetrahedra. Optical study shows a covalent character of Ni–O bonds.

### Acknowledgment

M. Chakir would like to thank the ICMCB Institute, France for their support.

### References

- [1] Y. Hasegawa, S. Tamura, N. Imanaka, G. Adachi, Y. Takano, T. Tsubaki, K. Sekizawa, J. Alloys Compd. 375 (2004) 212.
- [2] A. Aatiq, M. Menetrier, A. El Jazouli, C. Delmas, Solid State Ion. 150 (2002) 391.
- [3] T. Alami, R. Brochu, C. Parent, L. Rabardel, G. Le Flem, J. Solid State Chem. 110 (2) (1994) 350.
- [4] L.O. Hagman, P. Kierkegaard, Acta Chem. Scan. 22 (1968) 1822.
- [5] R. Masse, A. Durif, J.C. Guittel, I. Tordjman, Bull. Soc. Fr. Mineral. Crystallogr. 95 (1972) 45.
- [6] S. Krimi, A. El Jazouli, A. Lachgar, L. Rabardel, D. de Waal, J.R. Ramos-Barrado, Ann. Chim. Sci. Mater. 25 (1) (2000) 75.
- [7] S. Krimi, A. El Jazouli, D. de Waal, J.R. Ramos-Barrado, in: Proceeding of the Sixth ESG Conference, Montpellier, 2–6 June, 2002.
- [8] S. Krimi, I. Mansouri, A. El Jazouli, J.P. Chaminade, P. Gravereau, G. Le Flem, J. Solid State Chem. 105 (1993) 561.
- [9] J.P. Boilot, G. Collin, R. Comes, J. Solid State Chem. 50 (1983) 91.
- [10] R. Salmon, C. Parent, M. Vlasse, G. Le Flem, Mater. Res. Bull. 14 (1979) 85.
- [11] C. Masquelier, C. Wurn, J. Rodriguez-Carvajal, J. Gaubicher, L. Nazar, Chem. Mater. 12 (2000) 525.
- [12] J. Gaubicher, C. Wurn, G. Goward, C. Masquelier, L. Nazar, Chem. Mater. 12 (2000) 3240.
- [13] S. Barth, M. Andratschke, A. Feltz, C. Jager, Sci. Ceram. 14 (1989) 401.
- [14] F. Cherkaoui, Thesis, University of Bordeaux I, 1985.
- [15] M. Chakir, Thesis, University of Hassan II-Mohammedia, 2003.
- [16] A. Aatiq, Powder Diff. 19 (3) (2004) 272.
- [17] R.D. Shannon, Acta Crystallogr. A 32 (1976) 751.
- [18] N.E. Brese, M. O'Keeffe, Acta Crystallogr. B 47 (1991) 192.
- [19] S. Patoux, G. Rousse, J.B. Leriche, C. Masquelier, Chem. Mater. 15 (2003) 2084.
- [20] M. Chakir, A. El Jazouli, D. de Waal, in progress.
- [21] P. Tarte, A. Rulmont, C. Merckaert-Ansay, Spectrochim. Acta (A) 42 (9) (1986) 1009.
- [22] A. El Jazouli, M. Alami, R. Brochu, J.M. Dance, G. Le Flem, P. Hagenmuller, J. Solid State Chem. 71 (1987) 444.
- [23] A.B.P. Lever, Inorganic Electronic Spectroscopy, Elsevier, Amsterdam, 1984.